Chinese Chemical Letters 34 (2023) 107506

Contents lists available at ScienceDirect

Chinese Chemical Letters

journal homepage: www.elsevier.com/locate/cclet

DNA tetrahedron-based split aptamer probes for reliable imaging of ATP in living cells

Lie Li[1], Jie Wang[1], Huishan Jiang, Xiaohong Wen, Mei Yang, Suping Li, Qiuping Guo*, Kemin Wang*

State Key Laboratory of Chemo/Biosensing and Chemometrics, College of Biology, College of Chemistry and Chemical Engineering, Hunan University, State Key Laboratory for Bio-Nanotechnology and Molecular Engineering of Hunan Province, Changsha 410082, China

ARTICLE INFO

Article history:
Received 28 January 2022
Revised 20 April 2022
Accepted 9 May 2022
Available online 13 May 2022

Keywords:
Adenosine triphosphate
DNA tetrahedron
Split aptamer
Fluorescence resonance energy transfer
Living cell imaging

ABSTRACT

Accurate detection and imaging of adenosine triphosphate (ATP) expression levels in living cells is of great value for understanding cell metabolism, physiological activities, and pathologic mechanisms. Here, we developed a DNA tetrahedron-based split aptamer probe (TD probe) for ratiometric fluorescence imaging of ATP in living cells. The TD probe is constructed by hybridizing two split ATP aptamer probes (Apt-a and Apt-b) to a DNA tetrahedron assembled by four DNA oligonucleotides (T1, T2, T3 and T4). In the presence of ATP, the TD probe will alter its structure from the open to closed state, thus bringing the separated donor and acceptor fluorophores into close proximity for high fluorescence resonance energy transfer (FRET) signals. The TD probe exhibits low cytotoxicity, efficient cell internalization and good biological stability. Moreover, based on the FRET "off" to "on" signal output mode, the TD probe can effectively avoid false-positive signals from complex biological matrices, which is significant for long-term reliable imaging in living cells. In addition, by changing the split aptamers attached to DNA tetrahedron, the proposed strategy may be extended for detecting various intracellular targets. Collectively, this strategy provides a valuable sensing platform for biomarkers analysis in living cells, thus having great potential for early clinical diagnosis and therapeutic evaluation.

Adenosine triphosphate (ATP), a multifunctional molecule in living entities, plays vital regulatory roles in various biological processes [1–3]. A disordered ATP level is closely related to many serious diseases including hypoglycemia, Parkinson's disease, hypoxia, ischemia, and angiocardiopathy [4–6]. To date, many classic ATP detection methods have been explored [7–10], such as electrophoresis, high performance liquid chromatography, and chemiluminescence. However, these approaches are usually time-consuming, labor-intensive, and not suitable for *in situ* imaging of ATP in living cells [11,12]. Thus, engineering of a facile and reliable strategy for the real-time monitoring of intracellular ATP levels is of essential significance for clinical diagnosis and pathological analysis.

In recent years, the aptamer-based ATP sensors have received extensive attention owing to the benefits of aptamer-recognizing components, including high affinity, long-term stability, and ease of synthesis and modification [13,14]. Aptamers are single-stranded oligonucleotides capable of recognizing their specific targets [15–18]. A variety of aptamer sensors have been designed for ATP analysis by using different transduction models [19–23], such as fluorescence, colorimetry, and electrochemistry. Especially, the fluorescence-based detection has been widely applied in biological research due to its fast response and simple operation [19,20]. Nevertheless, at least two issues remain to be resolved when using aptamer-based fluorescent probes for ATP imaging in living cells. The first problem is the effective delivery of probes into the cell, a critical step for intracellular applications. The other is the biostability and biocompatibility of nucleic acid probes. Generally, a single nucleic acid probe is susceptible to degradation by intracellular nucleases, leading to inevitable false-positive signals [24,25]. To settle these problems, strategies incorporating exogenous nanomaterials (*e.g.*, graphene and polymers) have been developed for intracellular ATP imaging [26,27]. However, nanomaterials usually require complex preparation and functionalization steps, and even show some cytotoxicity to cells, which may interfere with the authentic expression level of ATP in living cells.

* Corresponding authors.
E-mail addresses: guoqping@hnu.edu.cn (Q. Guo), kmwang@hnu.edu.cn (K. Wang).
[1] These authors contributed equally to this work.

https://doi.org/10.1016/j.cclet.2022.05.020
1001-8417/

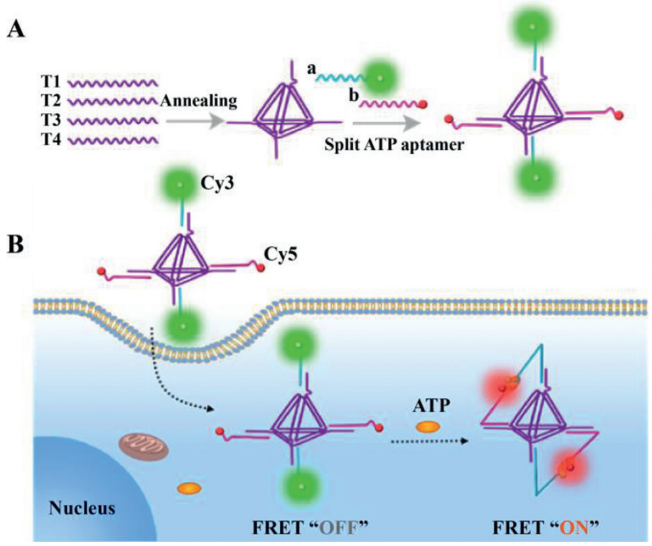

Scheme 1. (A) Construction and (B) schematic illustration of the TD probe for ratiometric fluorescence imaging of ATP in living cells.

DNA-based nanotechnology provides exciting opportunities to explore powerful biosensing strategies [28–32]. Especially, the DNA tetrahedron, an emerging nanophase biomaterial, exhibits several unique merits in the field of biology and medicine, such as excellent biocompatibility, nanoscale controllability, and editability [33–35]. Furthermore, it can be rapidly endocytosed into cells *via* a caveolin-dependent pathway, and maintain good stability within 48 h [36,37]. These capabilities have significantly facilitated its applications in bioimaging, logic computing and drug delivery [38–40]. For example, Xing *et al.* have developed an accelerated DNA tetrahedron based molecular beacon for efficient detection and imaging of miRNA in living cells [41]. Su *et al.* have reported the first example of vertebral-shaped DNA tetrahedron nanostructures for accurate cancer identification and miRNA silencing induced therapy [42]. Despite these progresses, most of them are single-intensity sensing modes, which are more prone to false-positive signals from complex biological matrices. As such, there is still an urgent need to develop an ingenious DNA tetrahedron-based fluorescent sensor for accurate intracellular imaging.

Inspired by the above challenges, we herein developed a DNA tetrahedron-based split aptamer probe (TD probe) for ratiometric fluorescence imaging of ATP in living cells, as illustrated in Scheme 1. The TD probe was composed of three modules: the DNA tetrahedron self-assembled by four DNA oligonucleotides (T1, T2, T3 and T4), the Cy3-labeled split ATP aptamer probe a (Apt-a) and the Cy5-labeled split ATP aptamer probe b (Apt-b). The DNA tetrahedron served as the backbone to immobilize two split aptamer probes *via* base complementary pairing. Meanwhile, the split aptamer probes as target recognition modules specifically bind to ATP molecules. In the absence of ATP, the fluorescent donor Cy3 and the fluorescent acceptor Cy5 were far apart due to the spatial separation of Apt-a and Apt-b, resulting in a low fluorescence resonance energy transfer (FRET) signal. In contrast, the presence of ATP will change the structure of the TD probe from the open to closed state, thus bringing the dual fluorophores into close proximity for high FRET signals. The proposed TD probe exhibited several unique properties, such as convenient preparation through a one-step procedure, excellent cell penetration and biological stability. Moreover, the FRET "off" to "on" signal output mode could effectively avoid false-positive signals from complex biological matrices, ensuring reliable ATP imaging in living cells.

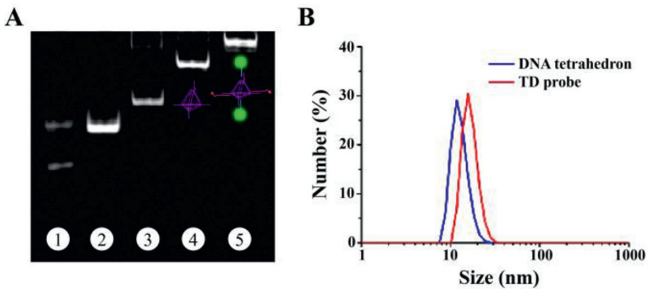

Fig. 1. (A) PAGE characterization of the TD probe. Lane 1: S1; lane 2: S1+S2; lane 3: S1+S2+S3; lane 4: S1+S2+S3+S4; lane 4: S1+S2+S3+S4+Apt-a+Apt-b. (B) DLS analysis of the DNA tetrahedron and TD probe.

The synthesis of the TD probe was first investigated *via* 6% polyacrylamide gel electrophoresis (PAGE). As shown in Fig. 1A, with the addition of DNA strands (lanes 1-4), the electrophoretic mobility gradually decreases due to the increase in the molecular weight of the hybridization complex, suggesting the construction of the DNA tetrahedron. Then, after mixing with Apt-a and Apt-b, an extended band with lower mobility appeared in lane 5, indicating the successful formation of the TD probe. In addition, the TD probe was also characterized by dynamic light scattering (DLS), where the average hydrodynamic diameters of the DNA tetrahedron and TD probe were approximately 12.1 nm and 16.1 nm, respectively (Fig. 1B). Moreover, atomic force microscopy (AFM) image revealed that the TD probe exhibited a good monodispersion (Fig. S1 in Supporting information). All these results clearly verified the successful assembly of the TD probe.

The feasibility of the TD probe for ATP detection was next investigated in a homogeneous solution. As shown in Fig. S2 (Supporting information), in the absence of ATP, a very weak FRET signal (F_A/F_D) of acceptor fluorophore (Cy5) to donor fluorophore (Cy3) was observed due to the spatial separation of Apt-a and Apt-b. Upon recognition of ATP, the TD probe showed a significant FRET signal, indicating that the designed TD probe was feasible for ATP sensing *in vitro*. Subsequently, real-time monitoring of the fluorescence emission intensity changes was performed to study the reaction kinetics. The excitation wavelength was fixed at 525 nm, and the emission wavelength was 667 nm (Fig. S3 in Supporting information). Without ATP, almost no change in fluorescence intensity was detected. Upon the addition of ATP, the fluorescence signal gradually increased and stabilized within 20 s, indicating that the TD probe could rapidly respond to the target. Then, the detection performance of the TD probe for ATP was investigated. As shown in Figs. 2A and B, the fluorescence spectra of the TD probe showed decreased Cy3 fluorescence at 560 nm and increased Cy5 fluorescence at 667 nm with the increasing ATP concentration from 0 to 3 nmol/L. Moreover, there was a good linear relationship between the FRET signal and ATP concentrations in the range of 0.02-0.2 mmol/L, and the limit of detection (LOD) was calculated to be 3.9 μmol/L ($R^2 = 0.962$) according to the blank signal plus 3σ (3 times the standard deviation). The performance of this strategy is better than some of the present nucleic acid-based fluorescence sensors [14,43]. The selectivity of the TD probe was also evaluated using three analogue molecules of ATP, including cytidine triphosphate (CTP), guanosine triphosphate (GTP), and uridine triphosphate (UTP). The FRET signal in the presence of ATP was higher than that of these ATP analogues (Figs. 2C and D), demonstrating the excellent specificity of the TD probe for ATP detection.

Good biological stability is quite important for DNA probes applied in complex physiological environment. To confirm the TD probe has good anti-degradation ability, the interaction of the TD probe with DNase I was first studied. As reported, DNase I is a

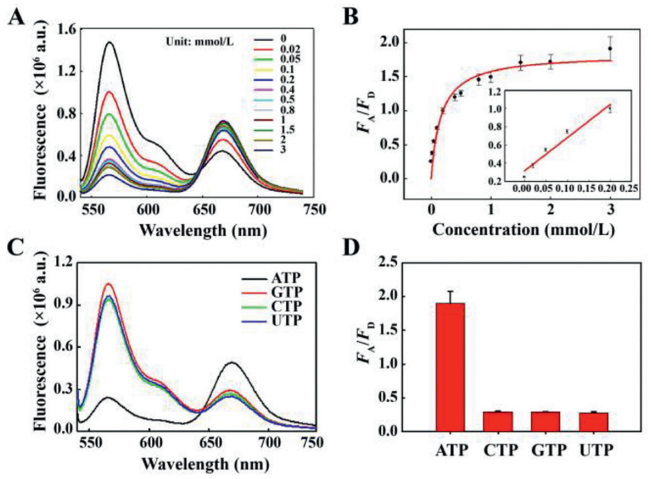

Fig. 2. (A) Fluorescence spectra of the TD probe in response to different concentrations of ATP. (B) The relationship between the FRET signal (F_A/F_D) and ATP concentration. The inset shows the linear relationship from 0.02 to 0.2 mmol/L. Fluorescence spectra (C) and FRET signal (D) of the TD probe in response to 2 mmol/L ATP, CTP, GTP and UTP, respectively.

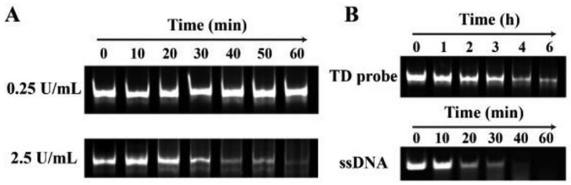

Fig. 3. (A) PAGE analysis of the low concentration of DNase I (0.25 U/mL) and high concentration of DNase I (2.5 U/mL) degradation assay products for the TD probe. (B) FBS (10%, v/v) degradation assay products for the TD probe and ssDNA at 37 °C.

powerful endonuclease that nonspecifically degrades single- and double-stranded DNA molecules by cleaving phosphodiester bonds [44,45]. The TD probe was respectively treated with 0.25 U/mL and 2.5 U/mL of DNase I for different times at 37 °C, then characterized by electrophoresis. As shown in Fig. 3A, almost no degradation was observed after incubation of the TD probe with 0.25 U/mL DNase I for 1 h, indicating that the TD probe had good biostability. However, after treatment with a higher concentration of DNase I (2.5 U/mL), the TD probe exhibited a time-dependent decrease in the electrophoretic band, and almost completely disappeared at about 50 min. Nevertheless, the FRET signal of the TD probe was not affected with the increase in the treatment time by 2.5 U/mL DNase I (Fig. S4 in Supporting information), which could avoid false-positive signals caused by nuclease degradation. The stability was further investigated by incubating TD probe with 10% (v/v) fetal bovine serum (FBS) (Fig. 3B). Compared with ssDNA probe, the TD probe exhibited longer-term stability, which was beneficial for intracellular bioimaging. Moreover, the biocompatibility of the TD probe was evaluated by the standard MTT (3-(4,5-dimethylthiazol-2-yl)-2,5-diphenyltetrazolium bromide) assay. After incubating with different concentrations of TD probes (0, 50, 100, 200 and 400 nmol/L) for 12 h at 37 °C, HeLa cells showed a good viability, with percentages over 88% (Fig. S5 in Supporting information). These results indicated that the TD probe was safe for cells and suitable for the following applications in living cells.

After demonstrating that the TD probe could achieve ATP sensing *in vitro*, we next explored its feasibility for ATP imaging in living cells. HeLa cells, which overexpressed ATP molecules, were selected as the research model. The cellular delivery ability of the TD probe was first investigated. As shown in Fig. 4, HeLa cells treated with free ssDNA probe showed very weak Cy3 and Cy5 fluorescence, suggesting that the free ssDNA probes were not suitable for ATP imaging in living cells due to their poor cell permeability and low biostability. In contrast, the cells incubated with the TD probe displayed obvious Cy3 and Cy5 fluorescence, indicating that the TD probe could be self-delivered into cells without any transfection agent, and used for ATP-imaging analysis in living cells. Then, the concentration and incubation time of the TD probe and HeLa cells were optimized for an optimal imaging performance. As shown in Fig. S6 (Supporting information), the FRET signal gradually increased during the incubation and reached saturated at about 4 h. Similarly, the FRET signal enhanced with increasing TD probe concentration and reached a maximal level at about 200 nmol/L (Fig. S7 in Supporting information). Therefore, 200 nmol/L TD probe and an incubation time of 4 h were chosen for subsequent experiments. Next, the intracellular distribution of the TD probe was examined. After incubating with the TD probe, HeLa cells were treated with the nuclear-specific dye Hoechst 33342 for 10 min at 37 °C. The imaging date showed that the Cy3 and Cy5 fluorescence was mainly distributed in the cytoplasm, which did not overlap with the blue fluorescence from Hoechst 33342, suggesting that the TD probe could be used for cytoplasmic ATP detection (Fig. S8 in Supporting information).

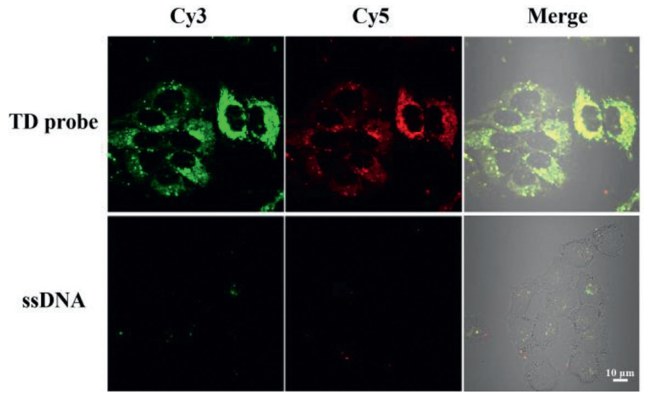

Fig. 4. Confocal fluorescence imaging of HeLa cells incubated with 200 nmol/L TD probe (top) and ssDNA (bottom) for 4 h at 37 °C.

To further confirm that the FRET signal was derived from endogenous ATP molecules in living cells, the TD probe was used to measure intracellular ATP changes upon different treatments. As reported, oligomycin can reduce intracellular ATP levels by inhibiting ATP synthase [46], and Ca^{2+} can increase intracellular ATP production *via* activating dehydrogenases [47,48]. Before incubating with the TD probe, HeLa cells were treated with 10 μmol/L oligomycin or 5 mmol/L $CaCl_2$ for 30 min at 37 °C. As shown in Fig. 5, compared with the control group (top), HeLa cells treated with oligomycin showed a decreased FRET signal (middle), while Ca^{2+}-treated cells exhibited a decreased FRET signal (bottom), indicating that the observed FRET signal was indeed associated with the intracellular ATP concentration. These results illustrated that the TD probe could dynamically monitor the changes of ATP in living cells.

In summary, combining DNA tetrahedron with split aptamers, we have successfully developed a TD probe for ratiometric fluorescence imaging of ATP in living cells. The TD probe is easily prepared by one-step incubation, and shows excellent specificity and high sensitivity for *in vitro* detection of ATP with a detection limit of 3.9 μmol/L. Moreover, the TD probe presents improved cell internalization efficiency, prominent resistance to nuclease degradation and satisfactory biocompatibility. More importantly, the FRET "off" to "on" signal output mode effectively avoids false-positive signals from complex biological matrices, which is critical for intracellular applications, especially for accurate imaging over long periods of time. Furthermore, by replacing the split aptamers attached to

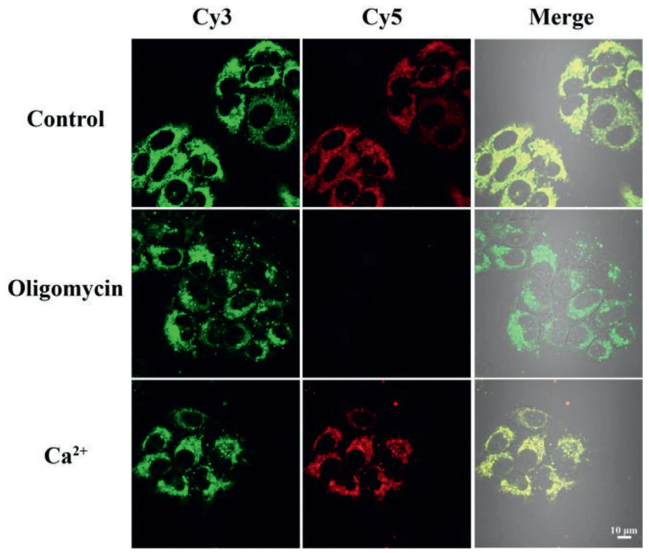

Fig. 5. Confocal fluorescence imaging of HeLa cells treated with medium (top), 10 μmol/L oligomycin (middle), and 5 mmol/L Ca^{2+} (bottom), followed by incubation with 200 nmol/L TD probe for 4 h at 37 °C.

DNA tetrahedron, the proposed strategy may be expanded to detect various intracellular targets. Thus, it provides a valuable sensing platform for accurate biomarkers analysis in living cells, which is of great significance for early clinical diagnosis and therapeutic evaluation.

Declaration of competing interest

The authors report no declarations of interest.

Acknowledgments

This work was supported by the Natural Science Foundation of China (Nos. 21877030, 21735002, 21778016 and 21521063).

Supplementary materials

Supplementary material associated with this article can be found, in the online version, at doi:10.1016/j.cclet.2022.05.020.

References

[1] S. Biswas, K. Kinbara, T. Niwa, et al., Nat. Chem. 5 (2013) 613–620.
[2] L. Lu, B. Li, S. Ding, et al., Nat. Commun. 11 (2020) 4192–4203.
[3] Y. Zhou, L. Zou, G. Li, et al., Anal. Chem. 93 (2021) 13960–13966.
[4] A.V. Gourine, E. Llaudet, N. Dale, et al., Nature 436 (2005) 108–111.
[5] B.S. Khakh, R.A. North, Nature 442 (2006) 527–532.
[6] Z. Duan, L. Tan, R. Duan, Anal. Chem. 93 (2021) 11547–11556.
[7] M.J. Gordon, X. Huang, S.L. Pentoney, et al., Science 242 (1988) 224–228.
[8] C. Fu, L. Song, Y. Fang, Anal. Chim. Acta 399 (1999) 259–263.
[9] F. Özogul, K.D.A. Taylor, P.C. Quantick, et al., Int. J. Food Sci. 35 (2000) 549–554.
[10] H. Huang, Y. Tan, J. Shi, et al., Nanoscale 2 (2010) 606–612.
[11] J. Dong, M. Zhao, Trends Anal. Chem. 80 (2016) 190–203.
[12] Y. Zhou, L. Yang, J. Wei, et al., Anal. Chem. 91 (2019) 15229–15234.
[13] S. Ng, H.S. Lim, Q. Ma, et al., Theranostics 6 (2016) 1683–1702.
[14] Y.X. Wang, D.X. Wang, J.Y. Ma, et al., Analyst 146 (2021) 2600–2608.
[15] L.C. Bock, L.C. Griffin, J.A. Latham, et al., Nature 355 (1992) 564–566.
[16] C.H.B. Chen, G.A. Chernis, V.Q. Hoang, et al., Proc. Natl. Acad. Sci. U. S. A. 100 (2003) 9226–9231.
[17] N. Lin, L. Wu, X. Xu, et al., ACS Appl. Mater. Interfaces 13 (2021) 9306–9315.
[18] L. Li, J. Wan, X. Wen, et al., Anal. Chem. 93 (2021) 7369–7377.
[19] X. Li, Y. Peng, Y. Chai, et al., Chem. Commun. 52 (2016) 3673–3676.
[20] X. Chai, Z. Fan, M.M. Yu, et al., Nano Lett. 21 (2021) 10047–10053.
[21] C. Li, M. Numata, M. Takeuchi, et al., Angew. Chem. Int. Ed. 44 (2005) 6371–6374.
[22] X. Zhang, C. Song, K. Yang, et al., Anal. Chem. 90 (2018) 4968–4971.
[23] X. Zuo, S. Song, J. Zhang, et al., J. Am. Chem. Soc. 129 (2007) 1042–1043.
[24] A.K. Chen, M.A. Behlke, A. Tsourkas, Nucleic Acids Res. 35 (2007) e105.
[25] L. He, D.Q. Lu, H. Liang, et al., ACS Nano 11 (2017) 4060–4066.
[26] F. Gao, J. Wu, Y. Yao, et al., RSC Adv. 8 (2018) 28161–28171.
[27] C.H. Zhang, H. Wang, J.W. Liu, et al., ACS Sens. 3 (2018) 2526–2531.
[28] L.Y. Duan, J.W. Liu, R.Q. Yu, et al., Biosens. Bioelectron. 177 (2021) 112976.
[29] D. Zhu, Y. Wei, T. Sun, et al., Anal. Chem. 93 (2021) 2226–2234.
[30] C. Zhu, J. Yang, J. Zheng, et al., Anal. Chem. 91 (2019) 15599–15607.
[31] J. Deng, J. Xu, M. Ouyang, et al., Chin. Chem. Lett. 33 (2022) 773–777.
[32] Z. Qing, J. Xu, J. Hu, et al., Angew. Chem. Int. Ed. 58 (2019) 11574–11585.
[33] Z. Zhou, Y.S. Sohn, R. Nechushtai, et al., ACS Nano 14 (2020) 9021–9031.
[34] Z. Qing, J. Hu, J. Xu, et al., Chem. Sci. 11 (2020) 1985–1990.
[35] L. Meng, W. Ma, S. Lin, et al., ACS Appl. Mater. Interfaces 11 (2019) 6850–6857.
[36] A.S. Walsh, H. Yin, C.M. Erben, et al., ACS Nano 5 (2011) 5427–5432.
[37] L. Liang, J. Li, Q. Li, et al., Angew. Chem. Int. Ed. 53 (2014) 7745–7750.
[38] J. Wang, D.X. Wang, J.Y. Ma, et al., Chem. Sci. 10 (2019) 9758–9767.
[39] Q. Lin, A. Wang, S. Liu, et al., Chem. Commun. 56 (2020) 5303–5306.
[40] X. Han, Y. Jiang, S. Li, et al., Nanoscale 11 (2019) 339–347.
[41] C. Xing, Z. Chen, Y. Lin, et al., Chem. Commun. 57 (2021) 3251–3254.
[42] J. Su, F. Wu, H. Xia, et al., Chem. Sci. 11 (2020) 80–86.
[43] X. Zheng, R. Peng, X. Jiang, et al., Anal. Chem. 89 (2017) 10941–10947.
[44] N. Li, M. Wang, X. Gao, et al., Anal. Chem. 89 (2017) 6670–6677.
[45] J.W. Keum, H. Bermudez, Chem. Commun. 45 (2009) 7036–7038.
[46] M.W. Bowler, M.G. Montgomery, A.G.W. Leslie, et al., Proc. Natl. Acad. Sci. U. S. A. 103 (2006) 8646–8649.
[47] E.J. Griffiths, G.A. Rutter, Biochim. Biophys. Acta 1787 (2009) 1324–1333.
[48] S. Hong, X. Zhang, R.J. Lake, et al., Chem. Sci. 11 (2020) 713–720.